Crack-Tip Damage and Fracture Toughness of Boron/Aluminum Composites

JONATHAN AWERBUCH

Department of Mechanical Engineering and Mechanics
College of Engineering
Drexel University
Philadelphia, PA 19104

AND

H. THOMAS HAHN*

Nonmetallic Materials Division
Air Force Materials Laboratory
Wright Patterson AFB, OH 45433

(Received January 29, 1979)

ABSTRACT

The fracture behavior of center notched unidirectional boron/aluminum composite under tensile loading has been investigated. Load-crack opening displacement (COD) curves were obtained for crack length-to-width ratios varying from 0.05 to 0.5. The COD was measured across the crack surfaces by means of the laser interferometric technique (gage length of 500 μm). As expected, the interferometric displacement gage (IDG) was found to be very sensitive to the appearance of damage at the crack tip, resulting in highly nonlinear load-COD curves. The damage at the crack-tip has been carefully examined by radiographs, SEM, photomicrographs, interferometric miscroscope and optical interferometry technique. Fracture strength results and experimental load-COD curves were compared with analytical predictions and an excellent agreement has been established. The resistance curve method has also been tried and found to be non-applicable. An understanding of the correlation between the observed failure modes and deformation characteristics has been achieved.

---

*Presently, University of California, Lawrence Livermore Laboratory, Livermore, CA 94550.

J. COMPOSITE MATERIALS, Vol. 13 (April 1979), p. 82

0021-9983/79/01 0082-26 $04.50/0

INTRODUCTION

BORON/ALUMINUM COMPOSITES have received most of the attention, among a variety of metal matrix composites, in the research activity and applications studies of recent years [1]. The mechanical behavior has been studied extensively during the past decade and results published in many reports and publications. An important subject of concern is the fracture behavior of boron/aluminum composites, which exhibit extremely low elongation up to fracture.The importance of understanding the fracture behavior of boron/aluminum can be demonstrated, for example, from the results of recent study on hard object impact damage of metal matrix composites [2]; the induced impact damage can be modeled as through-the-thickness cracks for post-impact residual strength predictions. In other words, the fracture behavior of unidirectional boron/aluminum composite with induced lateral impact damage is similar to the fracture behavior in the presence of artificial cracks and holes. Thus, understanding the behavior of the material in the presence of artificial notches is essential for design purposes.

A fair amount of work on the fracture behavior and toughness of boron/aluminum (B/Al) composites has been performed in recent years. The applicability of linear elastic fracture mechanics (LEFM) to unidirectional B/Al has been discussed in [3, 4, 5] with varying conclusions. For example, Kreider and Dardi [3], and Mar [4] concluded that the correlation between fracture strength σ_f and half crack length a is best described by an equation of the form $\sigma_f a^m$ = Const. However, contrary to LEFM predictions, the exponent m was found to be less than one half. Wright [5] concluded that LEFM can be applied, provided that the crack extension prior to failure is added to the initial crack length. With this assumption, the data of [5] as well as [3] do agree with predictions based on LEFM. This assumption does follow, in fact, the analytical models proposed in [6, 7] for notched strength predictions of composites. Hancock and Swanson [8] concluded that the conventional concepts of fracture toughness can be useful in characterizing the toughness of unidirectional B/Al. Sun and Prewo [9] showed that the fracture toughness of B/Al can be described by LEFM provided the crack extension is colinear with the initial pre-machined notch, as is the case of [90] or [0/90] laminate of compact tension specimen geometry. For unidirectional B/Al, such an approach is not relevant [9] due to the large amount of plastic deformation of the matrix parallel to the filaments. Similar damage growth and modes of failure under static and fatigue loadings have been observed and discussed in detail by many authors, e.g. [3, 10, 11, 12]. In general, it has been shown that the failure of unidirectional B/Al is preceded by longitudinal plastic deformation at the crack tip which eventually leads to matrix cracking and crack-tip blunting, all of which contribute to the crack arresting mechanism. The incipient matrix cracking has been described by the elastic stress intensity factor [10]. Obviously when different analytical approaches and experimental techniques are employed to define fracture toughness, the resulting toughness values vary significantly. However, most of the values are still very promising in comparison to other metal or resin matrix composites. Although many studies have been performed on the fracture behavior of B/Al composites, a definitive correlation between the observed failure modes and the deformation characteristics is lacking at this stage. Therefore, in the present paper, more emphasis is placed on the deformation behavior and the associated characterization methods.

Specifically, load-crack opening displacement (COD) curves are presented for center notch unidirectional 5.6 mil B/Al-6061-F specimens having crack length-to-width ratios ranging from 0.05 to 0.5. The COD was measured across the crack surface by means of laser interferometric technique. As expected, the Interferometric Displacement Gage (IDG) is found to be very sensitive to the appearance of crack tip damage, resulting in highly nonlinear load-COD curves.

The damage at the crack tip is examined by radiography, SEM, photomicrographs, interferometric microscope, and optical interferometry technique. Fracture strength data are analyzed and load-COD curves are compared with predictions, and an excellent agreement between theory and experiments is established. The resistance curve method was also tried to characterize the fracture resistance of the subject material but could not be applied. The results of this work, in conjunction with the results of a recent study [13] on the K-calibration of unidirectional metal matrix composites, gives a detailed description of the fracture behavior of unidirectional boron/aluminum.

EXPERIMENTAL PROCEDURE

Displacement Gages

The crack opening displacement (COD) was measured by means of laser interferometric technique which enables measuring displacement over a very short gage length. The COD was measured across the crack surface, at the center of the crack, with gage length of about 500 μm (0.02 in). This Interferometric Displacement Gage (IDG) was found to be highly sensitive in detecting crack-tip damage, very accurate in the submicron scale, and simple to utilize. As the Interferometric Displacement Gage (IDG) has not been used before for composite materials, it was also of interest to compare the load-COD curves with the load-displacement curves obtained by using standard compliance and clip gages, 1.0 and 0.25 inch gage length, respectively. A detailed description of the test procedure and experimental technique of both the IDG and clip gages is given in [13]. A comprehensive description of the laser interferometric technique is outlined in several papers published recently, e.g. [14, 15]. All tests were performed on the Instron testing machine at displacement rate of 0.005 inch/min.

Materials

The material tested is unidirectional boron/aluminum 6061-F (B/Al-6061-F) containing approximately 50% by volume 5.6 mil diameter boron filaments. The material was fabricated by United Technology Research Center by the "Quick Bond" process using the conditions of 550°C, 68.9 MPa, 10 min. in air. All specimens were cut from 5.5 × 5.5 inch plates, 0.052 inch thick (eight plies), parallel to the fibers' direction with a diamond saw or by E.D.M. (Electro Discharge Machining) method, and were ground on the edges to ensure minimum damage. The specimen dimensions were 14cm. long by 2.5cm. wide (5.5 in. by 1.0 in.). Center notches of about 0.05, 0.1, 0.2, 0.3, 0.4, 0.5 in. long and 0.01 in. wide were introduced by E.D.M. Aluminum doublers of 1.0 in. square were sheared from 0.05 in. thick 2024-T6 aluminum sheets and were glued with epoxy onto the specimen ends. A total of 16 center notch tension specimens were tested. Several unnotched specimens were tested statically to provide baseline strength data.

Failure Modes

A detailed study of the crack-tip damage growth and fracture surface has been performed by radiography, SEM, photomicrographs, interferometric microscope, and optical interferometry technique. Each specimen was loaded several times to a predetermined load, unloaded, and removed from the testing machine. Through photomicrographs the crack tip damage was carefully examined at the outer surface of the specimen, and the permanent opening of the crack was measured. The damage growth resulting from increasing load was also examined using the optical interferometry technique. The fracture surface was inspected through the SEM. For a few specimens the matrix was dissolved and the damage extension beyond the fracture surface was examined.

RESULTS AND ANALYSIS

Load-COD Curves

A typical load-COD curve obtained from the Interferometric Displacement Gage (IDG) is shown in Figure 1 for a B/Al specimen having initial crack length of 12.85 mm (0.504 in.). As seen in Figures 1 and 2, the load-COD curve is highly nonlinear, followed by rapid increase in COD when the load approaches its ultimate level. The rapid changes in COD have been found to be due to fiber failure, longitudinal plastic deformation, and longitudinal cracking of the matrix near the crack tip. This type of damage and plastic deformation at the crack tip is thus easily detected by monitoring the COD at the center of the crack.

The short gage length (500μm) of the IDG makes this technique more sensitive to the appearance of crack tip damage than the standard compliance gages, clip gages, or strain gages located at the crack tip. In fact, all previous load displacement curves obtained for unidirectional B/Al and other metal matrix and resin matrix composites are linear, as presented in numerous publications [16, 17, 18]. When the IDG is used, the crack tip damage is manifested in highly nonlinear load-COD

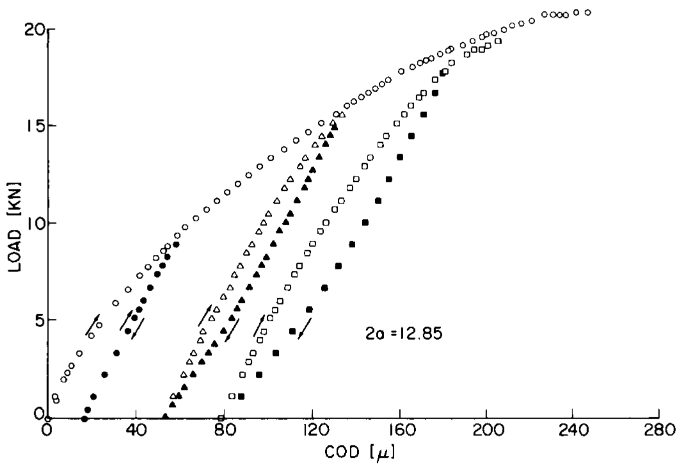

Figure 1. Load-COD (loading-unloading) curves obtained with interferometric displacement gage (crack length 12.85mm). The high nonlinearity and the large permanent COD remaining upon unloading indicate severe crack tip damage.

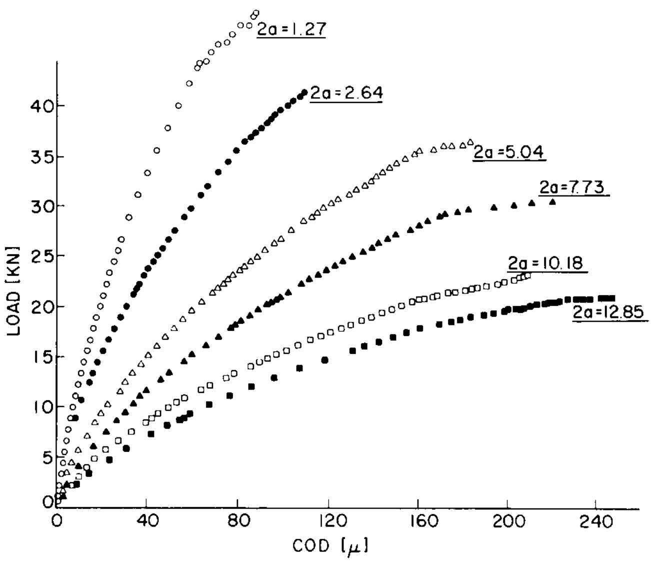

Figure 2. Load-COD curves for various crack sizes.

curves and a large permanent COD remaining upon unloading, as shown in Figure 1. To verify the accuracy of the large permanent displacement obtained with IDG technique, each specimen was removed from the testing machine after each unloading and the permanent opening of the crack was directly measured under a microscope. A comparison of the permanent displacement measured from the load-COD curves and from the direct measurements shows an excellent agreement for all specimens and for all load levels, demonstrating the accuracy of the IDG technique.

As the load approaches its ultimate level, the crack tip damage grows much more rapidly, causing the rapid increase in COD. Detailed examination of the load-COD curves also reveals a high nonlinearity between jumps in COD.

This high nonlinearity of the load-COD curve makes it difficult, and practically impossible, to measure the elastic compliance, and consequently to determine the stress intensity factor calibration curve. Therefore, in using the IDG technique, each specimen was loaded to a predetermined load and then unloaded. This procedure was repeated several times incrementally up to failure, as shown in Figure 1. Examining the load-COD curve (Figure 1) reveals that the unloading curve and the subsequent loading curve are initially linear. It is this linear portion of the load-COD curve that was used in [13] to obtain the compliance as a function of the initial crack length. Although the nonlinearity of the load-COD curves and the large permanent COD obtained with the IDG indicate the occurance of crack tip damage at relatively low load levels, this damage is subcritical and does not affect the compliance measurements. A detailed discussion of the compliance curves and the stress intensity factor calibration is given in [13].

Figure 1 also shows a "combined" load-COD curve, constructed by combining the individual loading-unloading curves. As seen in Figure 1, the overall load-COD behavior is very similar to that of metals. The effect of the crack length on the load-COD curve is shown in Figure 2. Here again the "combined" load-COD curves are shown for each crack length. Although the details of each curve cannot be seen in Figure 2, the nonlinearity, rapid increase in COD, and permanent opening upon unloading were obtained for every crack length tested. As expected, these characteristics are more pronounced as crack length increases; that is, the longer the original crack length, the larger the crack tip damage.

It may be noted that damage growth is accompanied by audible levels of acoustic emission. A recent study correlating the acoustic emission with damage growth detected through COD measurement for B/Al-1100 shows that a qualitative correlation can be found [19].

Fracture Strength

Table 1 lists the fracture strength data for various crack lengths. The average unnotched strength (of seven specimens) was relatively high; 2004 MPa (290.7 ksi) with standard deviation of 82.7 MPa (12.0 ksi). The average longitudinal stiffness was 245.5 GPa (35.6×10^3 ksi) with standard deviation of 14.8 GPa (2.15×10^3 ksi).

Table 1: Notched Strength of Unidirectional Boron/ Aluminum.

Crack Length [mm]	Crack Length [inch]	Notched Strength [MPa]	Notched Strength [ksi]
1.27	0.050	1537.7	222.30
1.35	0.053	1493.6	216.62
2.64	0.104	1282.1	185.95
2.64	0.104	1321.9	191.73
5.03	0.198	1112.1	161.30
5.23	0.206	1089.6	158.03
7.47	0.294	896.6	130.04
7.59	0.299	897.4	130.15
7.72	0.304	954.0	138.37
10.18	0.401	708.1	102.70
10.18	0.401	719.4	104.34
12.85	0.506	625.2	90.68
12.85	0.506	602.2	87.34

The notched strength of composite materials can be predicted by using the existing analytical model suggested by Waddoups, Eisenmann and Kaminski (WEK), [6]. They assumed the existence of intense energy regions at the edges of the notch which are modeled as edge cracks of size c_o. With this in mind, the linear elastic fracture mechanics is applied and the fracture strength can be predicted according to:

$$Y \frac{\sigma_f}{\sigma_o} = \left[\frac{c_o}{a + c_o} \right]^{1/2} \tag{1}$$

where σ_f and σ_o are the notched and unnotched strengths, respectively. $Y(2a/W)$ is the isotropic finite width correction factor and a is the half crack length.

For the finite width correction factor Y, the following expression has been chosen [20]:

$$Y = 1 + 0.1282\,(2a/W) - 0.2881\,(2a/W)^2 + 1.5254\,(2a/W)^3 \tag{2}$$

Note that the analytical prediction uses the isotropic width correction factor, Equation (2), because of its proven applicability to unidirectinal B/Al specimens of the geometry chosen in the present work [13].

A similar model has been mathematically formulated by Whitney and Nuismer (WN), [6, 7]. Here the assumption is that failure occurs when the average stress over a distance a_o, ahead of the crack tip, equals the unnotched strength. From this "average stress criterion" the fracture strength can be predicted as

$$Y \frac{\sigma_f}{\sigma_o} = \left[\frac{a_o/2}{a + a_o/2}\right]^{1/2} \tag{3}$$

By comparing both models (Equations (1) and (3)) it can be seen that they are identical ($a_o = 2c_o$). It should be noted that c_o (or a_o) can only be obtained experimentally by performing at least one fracture test, and must be determined for each composite system independently. Since c_o (or a_o) is assumed to be a material property, i.e. a quantity independent of crack size, rearranging Equation (1) will give c_o as the slope of the following equation:

$$a = c_o \left[\left(\frac{\sigma_o}{Y\sigma_f}\right)^2 - 1\right] \tag{4}$$

Figure 3 shows the results plotted according to the format of Equation (4). The solid line represents a least squares fit of c_o which was found to be 1.0mm (0.0396 in.). As seen in Figure 3, the use of a constant value for c_o for different crack lengths appears to be justified. Thus, the effect of crack size on notched strength can be described very well by Equation (1) with c_o = 1.0mm (Figure 4). Note that a significant notch sensitivity is observed for the unidirectional B/Al; the notched strength at $2a/W = 0.5$ is only 40% of the unnotched strength.

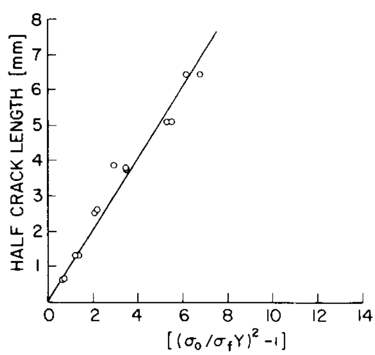

***Figure 3.** Least squares fit for c_o.*

Results obtained from [21] for the fracture strength data of unidirectional B/Al-6061 were analyzed as well. These B/Al composites were fabricated by Amercom Inc. through diffusion bonding, employing three different combinations of diffusion temperatures, pressures, and time. The details of fabrication procedure were not accessible to us, being the company proprietary information. Figure 5 shows the results of c_o for the three different materials. Again, the solid lines represent a least squares fit of c_o, and, as before, it seems that a constant value can be used. However, Figure 5 shows that each material has a different value of c_o. The numerical values of c_o for the three different B/Al are listed in Table 2.

As seen in Equation (1), smaller values of c_o indicate higher notch sensitivity, i.e., steeper change of $Y\sigma_f/\sigma_o$ with a. Thus, the conclusion should be that the fabrication procedure (pressure, temperature, and time of diffusion bonding

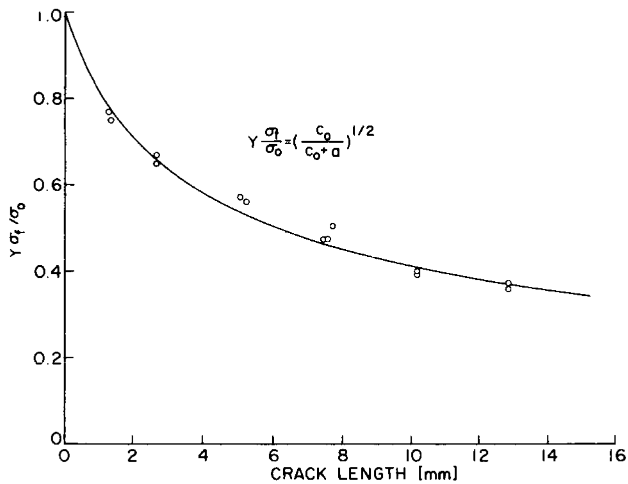

Figure 4. Comparison of analytical (WEK model) and experimental results for notched strength. Results show large notch sensitivity.

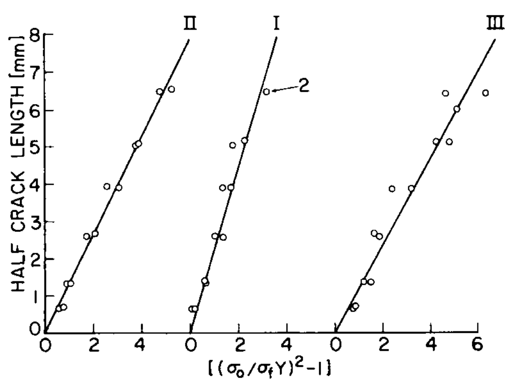

Figure 5. Least squares fit for c_o for various unidirectional B/Al composites. The fabrication procedure affects c_o.

procedure) does affect to some extent the notch sensitivity of B/Al composites. Values of the critical stress intensity factor, K_c obtained from the equation:

$$K_c = Y\sigma_f \sqrt{\pi(a+c_o)} = \sigma_o \sqrt{\pi c_o} \tag{5}$$

are also given in Table 2, indicating that the notch sensitivity depends, in fact, on the fabrication procedure. Figure 6 shows both experimental results and analytical

Table 2. Notched Strength Data

Material	σ_o Average MPa (ksi)	S.D.[a] MPa (ksi)	C.V.[b] %	K_c $MPa\sqrt{m}$ ($ksi\sqrt{in}$)	c_o mm (inch)
B/Al-present	2004 (290.7)	82.7 (12.0)	4.11	112.7 (102.6)	1.00 (0.0396)
B/Al-Type I	1290 (187.1)	60.1 (8.7)	4.67	107.3 (97.6)	1.15 (0.0455)
B/Al-Type II	1432 (207.7)	88.1 (12.8)	6.16	91.8 (83.5)	1.31 (0.0515)
B/Al-Type III	1526 (221.3)	65.7 (9.5)	4.31	91.9 (83.7)	2.20 (0.0867)

[a]Standard Deviation
[b]Coefficient of Variation

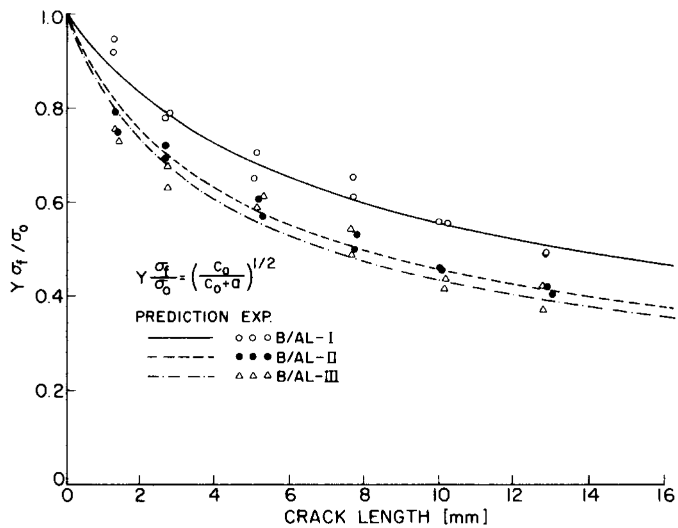

***Figure 6.** Effect of fabrication procedure on notch sensitivity. Best-fit curves (WEK model) are also shown.*

predictions, Equation (1), for the three different B/Al systems, based on c_o values of Table 2. The predictions represent the experimental results very well, except for the very short crack length of 0.05 in. That is, for B/Al type I, the model predicts higher strength than is actually observed, while the opposite holds true for B/Al types II and III.

As mentioned briefly in the introduction, another approach suggested by Mar and Lin (ML-model) [4] to analyze the fracture strength data is to assume

$$\sigma_f = M(2a)^{-m} \tag{6}$$

where M and m are determined so as to fit the data best. This model interprets m to be "the order of singularity of a crack lying in the matrix with its tip at the interface of matrix and filament." It was found in [4] that Equation (6) closely fits the data for $[\pm 45/0_2]$ B/Al, $[0/\pm 45]_{2s}$ graphite/epoxy [6], and $[0/\pm 45/90]_{2s}$ graphite/epoxy [7], and others. A similar model was presented in [22] and was supported experimentally in [3].

The data obtained in this program are plotted on log σ_f/σ_o versus log $2a/W$ format (Figure 7). A least squares fit yields the values of the slope m and of the coefficient M as 0.321 and 0.313, respectively, while the coefficient of correlation (c.c) is 0.971. As seen in Figure 7, Equation (6) follows the data quite closely. However, in order to compare both approaches, Equations (1) and (6), the WEK model is also plotted on the logarithmic format in Figure 8. A comparison of both Figures 7 and 8 reveals that the first model, Equation (1), does represent more accurately the notch sensitivity of unidirectional B/Al composites.

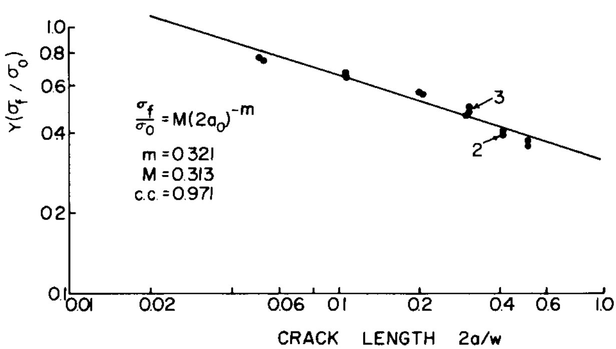

Figure 7. Experimental correlation for ML model.

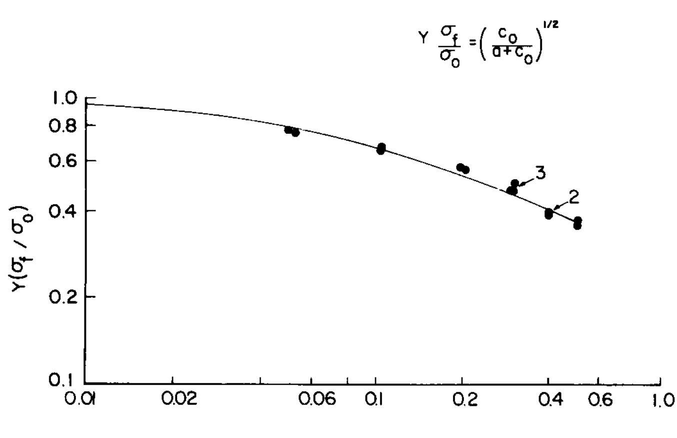

Figure 8. Experimental correlation for WEK model.

Crack-Tip Damage Growth and Failure Modes

As mentioned above, the rapid changes in COD are due to fiber failure at the crack tips which subsequently causes longitudinal plastic deformations and splitting in the matrix, shown in Figure 9a. This photomicrograph was taken after the specimen (crack length = 7.47 mm) was loaded up to 2.67 KN which is about 92% of its expected fracture strength. With increasing load, additional crack extension and additional longitudinal plastic zones are observed. The spacing between adjacent axial plastic zones equals approximately the fiber spacing. It should be noted that the length of the longitudinal plastic zones never extended beyond the specimens' gage length into the tabs. The final fracture surface is fairly irregular (Figure 9b, 10, 11b), resulting from a combination of the longitudinal plastic deformation of the matrix and the fracture of fibers at some weak spots along their lengths [11, 12]. This process repeats itself several times up to failure. The actual cracking of the matrix at the crack tip, Figure 10, did not take place during loading but only during the final stage of failure, probably because of the shock occurring during fracture. The splitting of the matrix runs through the entire thickness of the specimen, across the crack tip and around the fibers, Figure 9c. A view of the surface of the split matrix after fracture is shown in Figure 9d, revealing a large amount of shear plastic deformation.

It should be noted that the radius of the notch tip, resulting from the EDM of the notch, was relatively large (about 0.006 in.). However, it has been shown [3] that the effect of different radii at the notch tip (0.0023 and 0.005 in.) has little, if any, effect on the notched strength of unidirectinal B/Al, and even less effect when blunting of the crack tip is involved in the failure process, as is the case in our experiments.

The extension of the crack tip damage, as well as the number of longitudinal shear plastic zones, increases with load, as shown in Figure 12. These photographs were taken with an optical interferometry technique which enables measurement of the deformation zone immediately ahead of the crack tip [12]. In the present program, a collimated beam of monochromatic sodium vapor light ($\lambda = 0.5833 \mu m$) was directed through an optically flat quartz plate positioned directly on the polished specimen surface. During loading, the separation between the specimen's surface and the flat quartz plate, resulting from out-of-plate deformation at the crack tip, produces an optical interference pattern. No attempt has been made to obtain an optically flat surface, which is difficult to achieve because of the thinness of the specimens (0.052 in.) and the possibility of damaging the fibers immediately beneath the aluminum surface in polishing. Therefore, the quality of the pictures is not ideal [12], yet it is sufficient to identify the crack extension and the formation of new longitudinal plastic shear deformation bands of the matrix. As can be seen in Figure 12, the first longitudinal plastic deformation band is formed near the crack tip at relatively high load, about 80% of the notched strength. Crack extension then appears as the load increases further, and the whole process repeats itself.

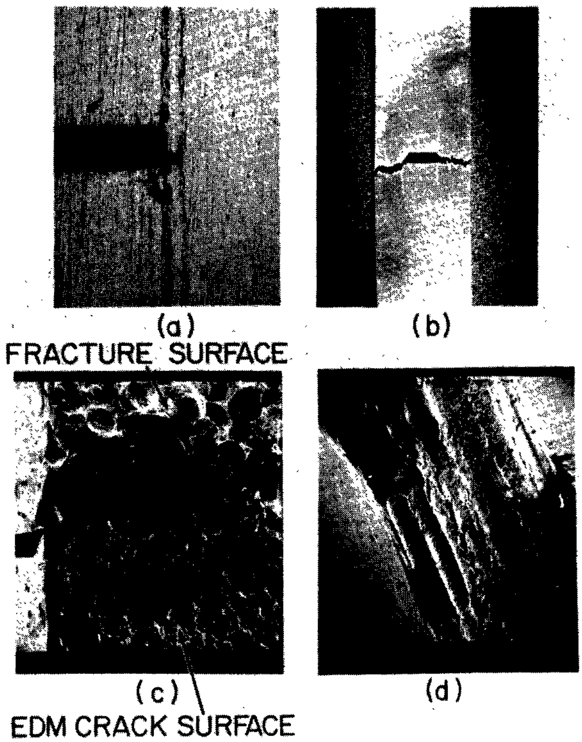

***Figure 9.** Crack tip damage growth and failure modes. a. Photomicrograph of crack tip damage showing crack extension and longitudinal plastic deformation. Crack length = 7.47mm. b. Photograph of fractured specimen showing matrix splitting at the crack tip. Crack length = 7.59mm. c. SEM view of matrix splitting at the crack tip. Crack length = 8.26mm. d. SEM side view of the split surface showing large amount of plastic deformation. Crack length = 7.72mm.*

***Figure 10.** Photomicrograph of crack tip damage after fracture. Multiple longitudinal plastic deformation of the matrix material extends to the specimen's edge.*

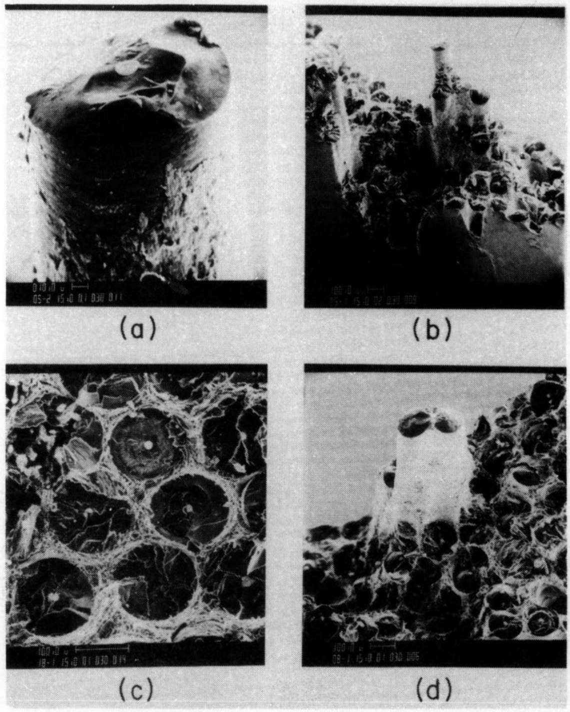

Figure 11. SEM photographs demonstrating good fiber-matrix and matrix-matrix bonding. a. Individual filament; b, c, d – Fracture surface.

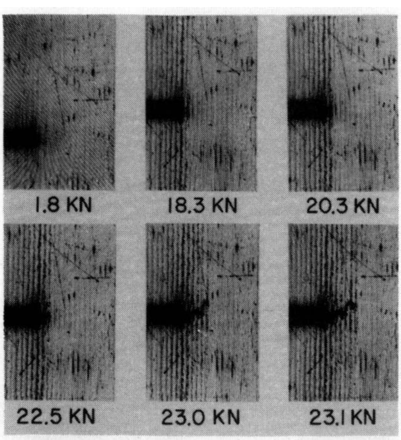

Figure 12. Optical interferometry photographs of B/Al (crack length = 8.26mm). under load. Crack extension and plastic zone increase with load.

Prior to fracture about 5 to 6 such shear yield zones were observed in several specimens of crack lengths varying from 0.3 to 0.5 inches. The plastic deformation of the matrix serves as a crack arresting medium, and additional crack extension alternates with the completion of successive longitudinal plastic deformation bands.

Many works studying the fracture behavior of unidirectional B/Al report that no slow crack growth actually occurs, but rather a sudden fracture is the typical failure mode. However, by properly polishing the test specimens and using the optical interferometry technique (or a standard interference microscope), stable crack tip damage growth can be detected as shown here. In fact, such an observation could be made through the load-COD curves as well. We also observed such stable damage growth for other metal matrix composite systems such as unidirectional borsic/titanium [23], B/Al-1100 [19], and B/Al laminate $[0/\pm22/0]_s$ [24]. Radiographs of preloaded specimens also confirmed this observation.

Since the spacing between adjacent plastic zones equals the fiber spacing, and since the matrix plastic deformation takes place prior to each crack extension (fiber failure), it is estimated that the total damage growth prior to failure (Δa) corresponding to 5 to 6 plastic zones at the crack tip amounts to about 0.7 to 0.8mm, in very good correlation with the estimated threshold crack extension given in [3]. Since the notched strength is mostly affected by the actual crack extension, it is of interest to compare this value (0.7 to 0.8mm) to the inherent flow size c_o in Equation (1) determined from the fracture strength results, Table 2. The comparison shows that c_o (= 1.0mm) is quite close to the actual extension of the crack Δa (= 0.7 to 0.8mm), while a_o in Equation (3) is quite different. Generally, the crack tip critical zone size c_o (or a_o), as introduced in [6, 7], is not based on the actual damage growth but is an empirical algebraic constant. However, it does serve very well its purpose of predicting the notched strength of unidirectional B/Al composites.

The damage growth, crack extension, and formation of longitudinal shear plastic zones depend also on the constituent properties, the interface properties, and the lay-up. For more ductile matrices, such as boron/aluminum-1100, the plastic deformation of the matrix was even observed at load levels as low as about 10% of the notched strength [19]. In such case, the crack arresting mechanism is more efficient and thus a lesser crack sensitivity is expected. Weak fibers combined with a strong, tough matrix seem to result in less notch sensitivity. For example, in borsic/titanium where the interphase effectively weakens the fibers considerably, notch sensitivity was found to be very small [23]. In B/Al laminate $[0/\pm22/0]_s$, crack blunting was negligible and a very high notch sensitivity was observed [24]. A detailed discussion on the metallurgical aspects of failure in B/Al composites is given, for example, in [25, 26].

The material tested in this program proved to be of high quality, having a very high longitudinal strength (2004 MPa). Scanning electron micrographs, Figure 12, indicate a very good fiber-matrix bond. Figure 12a shows a single fiber protruding from the matrix covered with a substantial residue of aluminum. Generally, the fibers are covered with residues of aluminum, Figure 12b, indicating a good fiber-matrix bond, i.e. the shear strength of the bond exceeds that of the aluminum matrix. Very little fiber pull-out has been observed. The few fibers shown in Figures 12b and 12d that have been pulled out of the opposite surface are exceptional and are shown here only to demonstrate the quality of the fiber-matrix bond. No matrix-matrix debonding has been observed, Figure 12c, and the large amount of microvoid formation (local yielding) seen appears to indicate the increased degree of triaxial restraint which occurs as the matrix-matrix bonding is enhanced [26]. The substantial shattering of the fibers, Figure 12c, as well as breaking of the tungsten core, is believed to be limited to a few fiber-diameters along the length of the fiber [23, 25, 26]. In some specimens the matrix material was dissolved in order to inspect the fibers in regions removed from the fracture surface. SEM inspections show that no multiple fiber failures have occurred in those regions.

Prediction of Load-COD Curves

The load-COD curve obtained by the IDG for various crack lengths, Figure 2, have been compared with an analytical model accounting for the longitudinal plastic deformations at the crack tip. As discussed earlier, the failure of notched unidirectional B/Al is preceded by crack tip blunting due to plastic shear deformation of the matrix in the filament direction. An analytical model predicting the length of the plastic zone, R_p, Figure 13, and the crack opening displacement at the crack tip (ΔV^p) has been suggested in [27, 28]. According to [28] the length of the plastic zone, R_p is

$$R_p = \frac{\pi^2}{16} \left[\frac{G_{LT}}{E_L}\right]^{1/2} \frac{aY^2P^2}{\tau_m{}^2 W^2 B^2} \tag{7}$$

and the corresponding permanent opening of the crack tip is:

$$\Delta V^p = \frac{8}{\pi} \left[\tau_m/(G_{LT}E_L)^{1/2}\right] R_p \tag{8}$$

where τ_m is the shear yield stress of the matrix and E_L and G_{LT} are the longitudinal and in-plane shear moduli, respectively. Note that ΔV^p predicts *crack tip* opening displacement (CTOD) but it can be compared to the COD at the *center* of the crack, measured experimentally, because it was found that the crack surfaces do not deform plastically during crack opening. Thus, combining Equations (7) and (8) we obtain

$$\Delta V^p = \frac{\pi}{4} \frac{1}{\tau_m E_L} \left(\frac{2a}{WB^2}\right) Y^2 P^2 \tag{9}$$

The elastic COD at the center of the crack, ΔV^e, has been shown to be [13]:

$$\Delta V^e = \frac{2\alpha Y}{E_L B} \frac{2a}{\mathrm{W}} P \tag{10}$$

where α is the orthotropic correction factor:

$$\alpha = \frac{1}{\sqrt{2}} \left[\left(\frac{E_L}{E_T} \right)^{1/2} - \nu_{LT} + \frac{E_L}{2G_{LT}} \right]^{1/2} \tag{11}$$

It has been shown [13] that the prediction of the elastic COD, Equation (10), agrees very well with the experimental results.

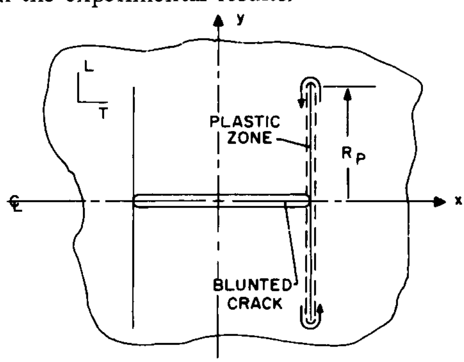

Figure 13. Blunted crack and longitudinal plastic zone.

The total crack opening displacement will be the sum of the elastic and plastic COD, i.e.:

$$\text{COD} = \Delta V^e + \Delta V^p = \frac{Y}{E_L B} \frac{2a}{W} \left[2\alpha + \frac{\pi Y}{4\tau_m W B^2} P \right] P \tag{12}$$

Equation (12) is compared very favorably with the experimental load-COD curves in Figure 14. The dashed lines in the Figures represent the initial slope of the load-COD curve as predicted from Equation (10). In order to achieve the good correlation between experiment and analytical model, the matrix shear yield stress τ_m was taken to be 207MPa (30ksi). In fact, the handbook data for boron/aluminum 6061-F give the value of 138MPa (20ksi) for τ_m. However, the tensile test data of the matrix material itself (fabricated of aluminum matrix alloy without the fiber reinforcement) show properties very close to aluminum 6061-T6 condition, which justify the choice of τ_m being equal to 207MPa (30ksi).

Coming back to Figure 14, we observe that the prediction deviates slightly from the experimental points at very low load levels. This is mainly due to the fact that the analytical model, Equation (12) predicts the formation of the longitudinal plastic shear deformation, and thus blunting of the crack tip, immediately upon initial loading. However, the first axial plastic zone actually appears at a much later

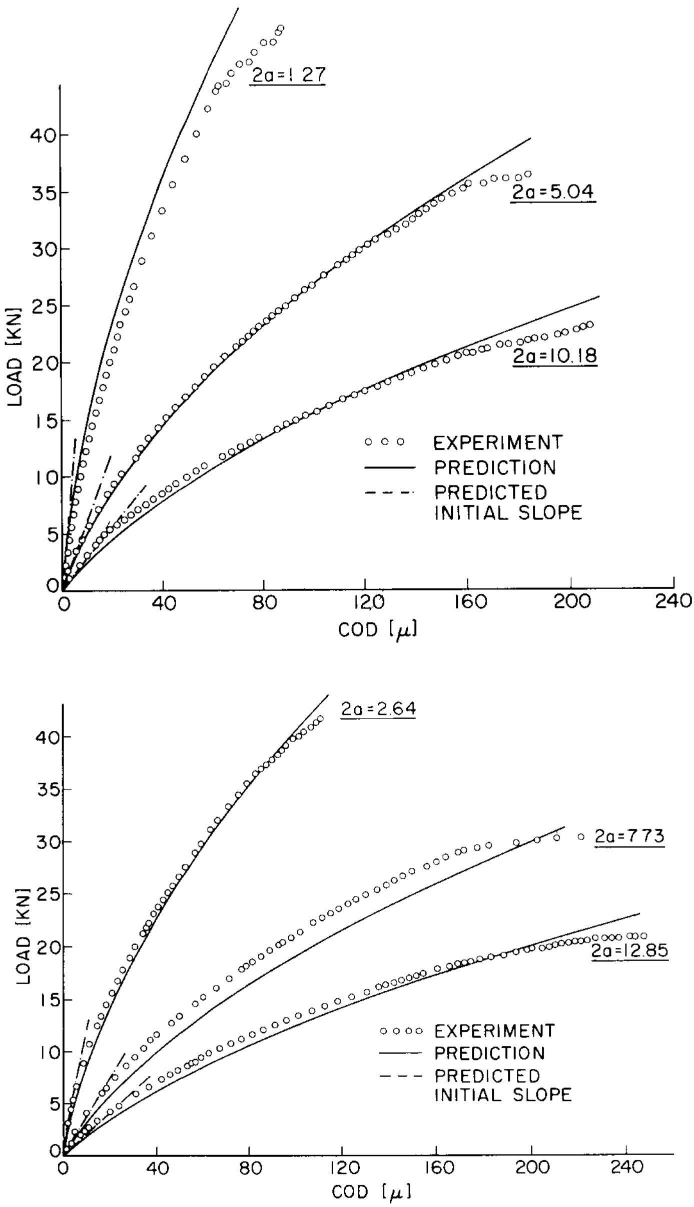

Figure 14. *Comparison of experimental and analytical results of load-COD curves for various crack lengths*

stage of the loading, as shown in Figure 12. The deviation of the prediction from the experimental data becomes more pronounced at higher load levels because the analytical model incorporates only one plastic zone, while at least 5 to 6 such zones are actually observed prior to failure, Figure 12. Therefore, Equation (12) predicts smaller crack openings than are actually observed as the load approaches its ultimate level.

As explained previously, after each intermediate loading, specimens were removed from the testing machine and the permanent opening of the crack was measured. The permanent opening of the crack was also determined from the loading-unloading curves, Figure 1. The experimental results of the permanent COD are compared with the prediction, Equation (9), as shown in Figure 15. The crack opening is given here in a nondimensional form in order to include results for the various crack sizes. The agreement between prediction and experiment is not as good, mainly because the prediction accounts for only one axial plastic zone rather than the multiple zones observed experimentally. However, the general trend of the data is very similar to the prediction.

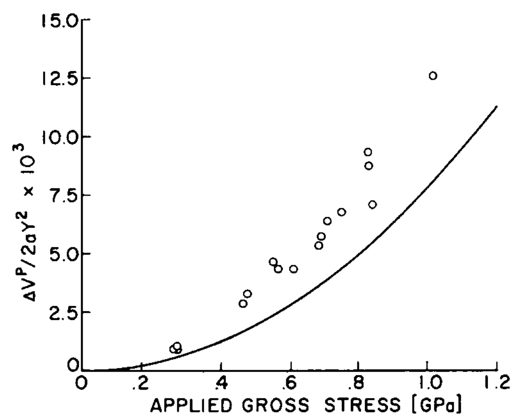

Figure 15. Comparison of experimental and analytical results of permanent COD as a function of applied load.

Resistance Curve Method

The resistance curve (K_R-Curve) method has been widely used to successfully characterize the fracture resistance of metals, e.g. [29, 30]. Application of this method to composites hinges on the assumption that the crack tip damage can be modeled as a self-similar crack extension and the effective crack length is determined through compliance matching. The question arises whether the resistance curve method can be applied to composite materials for which the damage growth can not be characterized as self-similar crack extension. Note that damage growth in composite laminates appears in the form of matrix cracking along the filament direction within individual plies, delamination, fiber breaks at weak locations, fiber-matrix debonding, etc. Obviously, the damage growth for unidirectional B/Al, as shown in this work, can-hardly be characterized as self-similar crack extension. However, there have been some attempts to apply the resistance curve method to composites on the basis of compliance matching. Gaggar and Broutman [31] concluded that the K_R-curve concept can be adopted for epoxy and polyester composites randomly reinforced with discontinuous fibers. Morris and Hahn [17] applied the resistance curve method to $[0/\pm 45]_s$, $[0/\pm 45]_{2s}$, and $[0/90/\pm 45]_s$ graphite/epoxy laminates, and they concluded that the K_R-curve can provide full information on the fracture resistance up to final failure. However, the results given in [17] indicate that the maximum value of K_R, as well as the amount of crack extension at failure, are not constant, and depend on the original crack length. Underwood [12] measured the out-of-plane deformation at the crack tip and the crack extension prior to failure using optical interferometry technique for single edge notched B/Al specimens. Using the K-calibration formula [20] for this geometry, the mode I stress intensity factor K_I was calculated and plotted against Δa. The data show a linear relationship between K_I and Δa for three different lay-ups: $[0°]$, $[0°/90]$, and $[+60°/0°/-60°]$.

Another objective of this program is thus to investigate the applicability of the resistance curve approach to unidirectional B/Al composite. In particular, the effects of the test technique employed (IDG versus compliance gage) and of the loading history are studied.

The detailed procedure of plotting the resistance curve is well established and is given in details in [17, 29, 30] and will not be repeated in full here. Briefly, a straight line is drawn from the origin to a selected point of the load-COD curve, Figure 2, and the compliance is measured from the inverse of the secant slope. The value of this compliance is matched on the compliance curve (calibration curve) obtained for this material (see Figures 11 and 12 of Ref. [13]) and the effective crack length ($a_{eff} = a_o + \Delta a$) is determined. Repeating this procedure, the different values of the effective crack length as a function of the load are obtained. It should be emphasized here that the effective half crack length a_{eff} is not a pre-existing crack and Δa is not necessarily the actual self-similar crack extension, but it is some damage growth which can be modeled, through the compliance matching, as self-similar crack extension. The crack growth resistance K_R is obtained from:

$$K_R = Y\sigma_f \sqrt{\pi a_{eff}}\ ; a_{eff} = a_o + \Delta a \tag{13}$$

A typical K_R-curve obtained for center notch unidirectional B/Al is depicted in Figure 16. Three different K_R-curves are shown in the Figure:

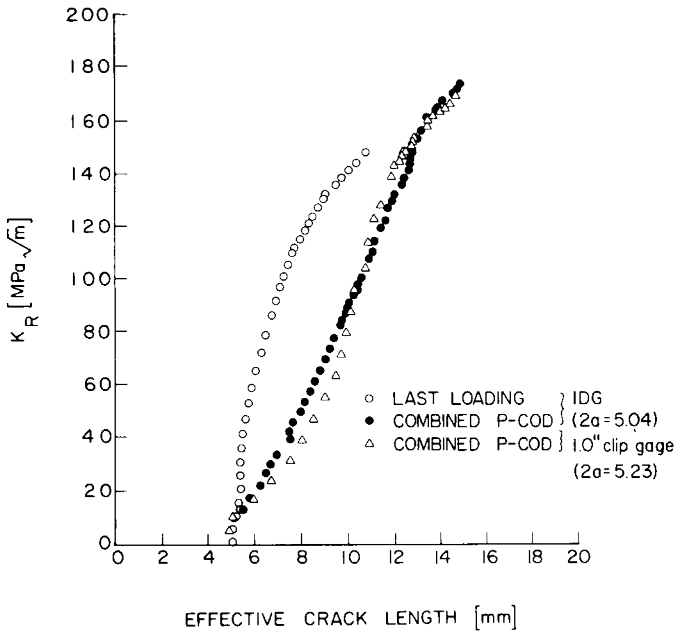

Figure 16. Fracture resistance data obtained from the IDG and compliance gage techniques.

(1) K_R-curve obtained from the "combined" load-COD curve, using the *local* compliance curve, Figure 12 of [13]—closed circles.

(2) K_R-curve obtained from "Last" Load-COD curve, using the *local* compliance curve, Figure 12 of [13]—open circles. Prior to last loading, the specimen was loaded to about 92% of its notched strength.

(3) K_R-curve obtained from load-displacement curve (compliance gage), using the *global* compliance curve, Figure 11 of [13]—open triangles.

All three curves are for 0.2 inch crack length. Comparing all three K_R-curves the following conclusions can be made:

1. The K_R-curve obtained by using the "combined" load-COD curve shows damage growth at a very early stage of the loading, due to the nonlinearity of the load-COD curve.

2. The K_R-curve obtained by using the "last" load-COD curve shows extension of damage at a much later stage of the loading. This is, however, misleading since some damage growth does exist prior to the "last" loading. Therefore, the maximum K_R is much smaller than the maximum value obtained from the "combined" load-COD curve.

3. The K_R-curve obtained by using the load-displacement curve (open triangles)

is very similar to the K_R-curve obtained by using the "combined" load-COD curve. This point, however, is not conclusive because such an agreement has not been observed for other crack lengths.

4. The point of instability of the critical fracture toughness K_C is defined by the point of tangency between K_R-curve as found from Equation (13), and the K_R-curve defined by

$$K_R = Y\sigma\sqrt{\pi a} \tag{14}$$

with σ as a parameter [29, 30]. Such a point of tangency could not be defined here; thus the last point on the K_R-curve defines K_C.

5. Comparison of the values of K_C from Figure 16 (K_C = 175MPa $\sqrt{m}$) and from Table 2 (K_C = 112.7MPa $\sqrt{m}$) shows a significant difference. The reason for this difference is mostly because the damage growth Δa used in Equation (13) is much longer than c_o as determined from the best-fit of the notched strength data, Figure 4. In fact, we could anticipate such a difference directly from the loading-unloading curves and the mode of crack tip damage growth. The longitudinal plastic deformation at the crack tip causes significant increase in COD, resulting in a large plateau in the load-COD curve.

6. Because of such a flat load-COD curve, using the compliance matching method for notches longer than 0.2 in. resulted in effective crack lengths which are longer than the width of the specimen! This is, of course, impossible. In other words, the K_R-curve cannot be applied to materials exhibiting the damage growth characteristic of unidirectional B/Al, and the assumption of "self similar crack extension" can not be applied when a sensitive displacement gage (such as the IDG) is employed.

7. It should be remembered that the change of the secant slope in the load-COD curve does not represent the actual crack extension. Since there remains permanent crack tip deformation upon unloading, Figure 1, the actual crack extension can be better characterized in terms of the change in the elastic compliance obtained from incremental loading-unloading curves. When this is done, a more reasonable K_R-curve will result for all crack lengths.

Figure 17 shows the K_R-curve obtained for the various initial crack lengths from the load-displacement curves (compliance gage). As this method is not as sensitive to damage growth as the IDG is, K_R-curves could be obtained for all crack lengths. The conclusions from Figure 17 are as follows:

1. The maximum K values measured from the K_R-curves are much higher than predicted using the WEK model, Equation (1).

2. The damage growth Δa is much longer than c_o and is not constant, as was also found in [17] for graphite/epoxy laminates. The maximum K values are not constant and depend on the initial crack length.

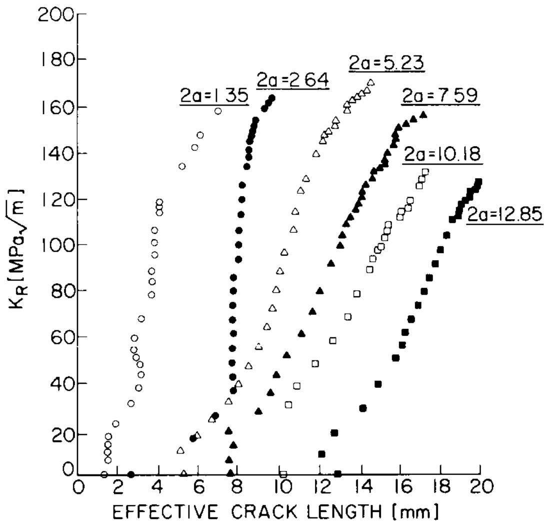

Figure 17. Fracture resistance data for various crack lengths obtained with compliance gage.

CONCLUSIONS

Load-crack opening displacement (COD) curves were obtained for crack length-to-width ratios varying from 0.05 to 0.5. The COD was measured across the crack surfaces by means of the laser interferometric technique. This technique was found to be highly sensitive in detecting crack tip damage, very accurate on the submicron scale, and simple to utilize.

The load-COD curves for center notched unidirectional boron/aluminum are highly nonlinear. Upon unloading, a relatively large permanent crack opening displacement remains, mainly because of the plastic deformation of the matrix at the crack tip. Such a correlation between the observed damage growth and deformation characteristics could not be confirmed using the standard compliance or clip gages.

The fracture strength of the material can be predicted by using the existing analytical models based on the concept of a critical damage zone size c_o at the crack tip being a material parameter. It has been determined that this damage zone size, obtained from the best fit of the data, agrees reasonably well with the observed damage growth, but it is much different from the damage size determined by using the resistance curve method. However, the notch strength data obtained for B/Al are in good agreement with predictions. Another proposed model, in which $r^{-1/2}$ singularity is not assumed, does not follow the experimental data as well.

The load-COD curves obtained by the IDG method have been compared with an analytical model. The model incorporates the longitudinal plastic deformation which eventually leads to cracking of the matrix. An excellent agreement is established between predictions and experiments for all the crack sizes tested.

A detailed study of the damage growth and failure mode indicates that the crack tip damage appears in the form of plastic deformation of the ductile matrix in the longitudinal direction. Prior to failure, multiple longitudinal plastic zones appear, accompanied by crack extension. The severity of the crack tip damage is demonstrated by the high nonlinearity of the load-COD curve, by the large amount of COD, and by the large permanent displacement remaining upon unloading. The resistance curve method has also been tried. However, it was found that the resistance curves depend strongly on the test method (IDG versus compliance gage) as well as the loading history. The calculated stress intensity factor and effective increment of crack length, both at fracture, were found to depend on the initial crack length.

It appears that the fracture behavior of the subject composite material under uniaxial static tension can be predicted. Also, the test procedure employed in this study is very helpful in better understanding the fracture behavior of composite materials. However, it seems that a full characterization of the fracture behavior of composite materials depends strongly on the test procedure and the mode of failure, and that a specific analytical approach has to be employed for each material system.

ACKNOWLEDGMENTS

The work of the first author (J. Awerbuch), performed at the Air Force Materials Laboratory (AFML), Wright Patterson AFB, Ohio, was supported in part by the National Research Council through the Resident Research Associateship Program and in part by the Metal and Ceramic Division of AFML through contract No. F33615-76-C-5124 with the University of Dayton Research Institute.

Special thanks are due T. Nicholas of AFML for implementing this program and for high technical assistance and encouragement. The support of S.W. Tsai in our research program is also acknowledged with appreciation.

The authors wish to express sincere gratitude to Messrs. R. Klinger and C. Bell for their help in the experimental program. Special thanks go to Mr. D.E. Macha for his guidance in the use of the laser interferometric test method. The help of J.W. Jones, of the University of Michigan in applying the optical interferometry technique is deeply appreciated.

REFERENCES

1. E. L. Foster, Jr., "Technology Development of Metal Matrix Composites to DOD Application Requirements," proceeding of First MMC Workshop, Institute of Defense Analysis, paper P-1144, September 1975.
2. J. Awerbuch and H. T. Hahn, "Hard Object Impact Damage of Metal Matrix Composites," *J. Composite Materials*, Vol. 10 (1976), p. 231.
3. K. G. Kreider and L. Dardi, "Fracture Toughness of Composites," *Failure Modes in*

Composites, I. J. Toth Edt., The Metallurgical Society of the AIME, Vol. I, New York, New York, 1972, p. 193.

4. J. W. Mar and K. Y. Lin, "Fracture Mechanics Correlation for Tensile Failure of Filamentary Composites With Holes," *J. of Aircraft*, Vol. 14 (1977), p. 703.
5. M. A. Wright and F. A. Iannuzzi, "The Failure of Notched Specimens of Boron-Fiber Reinforced 6061 Aluminum Alloy," *Failure Modes in Composites*, J. N. Fleck and R. L. Mehan, Eds., The Metallurgical Society of the AIME, Vol. II, New York, New York, 1974, p. 68.
6. M. E. Waddoups, J. R. Eisenmann and B. E. Kaminski, "Macroscopic Fracture Mechanics of Advanced Composite Materials," *J. Composite Materials*, Vol. 5 (1971), p. 446.
7. R. J. Nuismer and J. M. Whitney, "Uniaxial Failure of Composite Laminates Containing Stress Concentrations" in Fracture Mechanics of Composites, ASTM STP 593, American Society of Testing and Materials, 1975, p. 117.
8. J. R. Hancock and G. D. Swanson, "Toughness of Filamentary Boron/Aluminum Composites," *Composite Materials: Testing and Design* (Second Conference), ASTM STP 497, American Society for Testing and Materials, 1972, p. 299.
9. C. T. Sun and K. M. Prewo, "The Fracture Toughness of Boron Aluminum Composites," *J. Composite Materials*, Vol. 11 (1977), p. 164.
10. W. R. Hoover and R. E. Allred,"The Toughness of Borsic-Aluminum Composites With Weak Fiber Matrix Bonds," *Failure Modes in Composites*, I. J. Toth Edt., The Metallurgical Society of the AIME, Vol. I, New York, New York, 1972, p. 311.
11. K. M. Prewo and K. G. Kreider, "Fatigue Failure Mechanism in Boron Aluminum," *Failure Modes in Composites*, I. J. Toth Edt., The Metallurgical Society of the AIME, Vol. I, New York, New York, 1972, p. 395.
12. J. H. Underwood, "Crack-Tip Deformation Measurements Accompanying Fracture in Fibrous and Laminar Composites," *Composite Materials: Testing and Design* (Third Conference), ASTM STP 546, American Society for Testing and Materials, 1974, p. 376.
13. J. Awerbuch and H. T. Hahn, "K-Calibration of Unidirectional Metal Matrix Composites," *J. Composite Materials*, Vol. 12 (1978), p. 222.
14. D. E. Macha, W. N. Sharpe Jr., and A. F. Grant Jr., "A Laser Interferometry Method for Experimental Stress Intensity Factor Calibration," *Cracks and Fracture*, ASTM STP 601, American Society for Testing and Materials, 1976, p. 490.
15. W. N. Sharpe Jr., "Interferometric Surface Strain Measurements," *International J. Nondestructive Testing*, Vol. 3 (1971), p. 56.
16. J. P. Waszcak, "Applicability of Linear Elastic Fracture Mechanics to 5.6 mil. Boron/6061 Aluminum," *J. Aircraft*, Vol. 13 (1976), p. 770.
17. D. H. Morris and H. T. Hahn, "Fracture Resistance Characterization of Graphite/Epoxy Composites," *Composite Materials: Testing and Design* (Fourth Conference), ASTM STP 617, American Society for Testing and Materials, 1977, p. 5.
18. I. M. Daniel, R. E. Rowlands and J. B. Whitside, "Deformation and Failure of Boron/Epoxy Plate with Circular Holes," *The Test Methods for High Modulus Fibers and Composites*, ASTM STP 521, American Society for Testing and Materials, 1973, p. 143.
19. J. Awerbuch, "Failure Mechanism and Deformation Characteristics of Unidirectional Boron Aluminum Composites," to be published.
20. W. F. Brown and J. E. Srawley, in *Plane Strain Crack Toughness Testing of High Strength Metallic Materials*, ASTM STP 410, American Society for Testing and Materials, 1966.
21. R. L. Crane, Nondestructive Evaluation Branch at the Air Force Materials Laboratory, Wright Patterson AFB, Ohio, 45433. Private Communication.
22. E. M. Wu, in *Composite Materials Workshop*, S. W. Tsai, J. C. Halpin and N. J. Pagano, Eds., Technomic Publishing Co., Inc., 1968.
23. J. Awerbuch and H. T. Hahn, "Crack-Tip Damage and Fracture Toughness of Borsic/Titanium Composite," to be published.

24. J. Awerbuch, "Notch Sensitivity of Boron Aluminum Laminate," to be published.
25. R. C. Jones, "Fractography of Aluminum-Boron Composites," *Composite Materials: Testing and Design* (First Conference), ASTM STP 460, American Society for Testing and Materials, 1969, p. 512.
26. R. C. Jones and J. L. Christian, "Analysis of an Improved Boron/Aluminum Composite," *Composite Materials: Testing and Design* (Second Conference), ASTM STP 497, American Society for Testing and Materials, 1972, p. 439.
27. J. Tirosh, "The Effect of Plasticity and Crack Blunting on the Stress Distribution in Orthotropic Composite Materials," *J. Appl. Mech.*, Vol. 40 (1973), p. 785.
28. F. A. McClintock, "Problems in Fracture of Composites with Plastic Matrices," presented at the Fourth Symposium on High Performance Composites at St. Louis, MO., Monsanto Co. and Washington University, 1969.
29. *Fracture Toughness Evaluation by R-curve Methods*, ASTM STP 527, American Society for Testing and Materials, 1973.
30. J. Eftis, D. L. Jones and H. Liebowitz, Fracture Mechanics of Aircraft Structures, H. Liebowitz, Ed., AGARD-AG-176, North Atlantic Treaty Organization, 1974, p. 32.
31. S. Gaggar and L. J. Broutman, "Crack Growth Resistance of Random Fiber Composites," *J. Composite Materials*, Vol. 9 (1975), p. 216.

